Czechoslovak Mathematical Journal

Catarina P. Avelino; Altino F. Santos

Geometric and combinatorial structure of a class of spherical folding tessellations – I

Czechoslovak Mathematical Journal, Vol. 67 (2017), No. 4, 891–918

Persistent URL: http://dml.cz/dmlcz/146956

Czechoslovak Mathematical Journal, 67 (142) (2017), 891–918

GEOMETRIC AND COMBINATORIAL STRUCTURE OF A CLASS OF SPHERICAL FOLDING TESSELLATIONS – I

Catarina P. Avelino, Altino F. Santos, Vila Real

Received November 11, 2015. First published October 19, 2017.

Abstract. A classification of dihedral folding tessellations of the sphere whose prototiles are a kite and an equilateral or isosceles triangle was obtained in recent four papers by Avelino and Santos (2012, 2013, 2014 and 2015). In this paper we extend this classification, presenting all dihedral folding tessellations of the sphere by kites and scalene triangles in which the shorter side of the kite is equal to the longest side of the triangle. Within two possible cases of adjacency, only one will be addressed. The combinatorial structure of each tiling is also analysed.

Keywords: dihedral f-tiling; combinatorial propertie; spherical trigonometry; symmetry group

MSC 2010: 52C20, 52B05, 20B35

1. Introduction

By a *folding tessellation* or *folding tiling* (f-tiling, for short) of the sphere S^2 we mean an edge-to-edge pattern of spherical geodesic polygons that fills the whole sphere with no gaps and no overlaps, and such that the "underlying graph" has even valency at any vertex and the sums of alternate angles around each vertex are π.

Folding tilings are strongly related to the theory of isometric foldings on Riemannian manifolds. In fact, the set of singularities of any isometric folding corresponds to a folding tiling. See [13] for the foundations of this subject.

The study of this special class of tessellations was initiated in [5] with a complete classification of all spherical monohedral folding tilings. Ten years later, Ueno and Agaoka in [14] established a complete classification of all triangular spherical monohedral tilings (without any restriction on angles).

This research was partially supported by Fundação para a Ciência e a Tecnologia (FCT) through projects UID/MAT/00013/2013 and UID/Multi/04621/2013.

DOI: 10.21136/CMJ.2017.0610-15

Dawson has also been interested in special classes of spherical tilings, see [10], [11], [12], for instance.

A complete classification of all spherical f-tilings by rhombi and triangles was obtained in 2005, see [9]. A detailed study of triangular spherical folding tilings by equilateral and isosceles triangles is presented in [8]. Spherical f-tilings by two noncongruent classes of isosceles triangles have been recently obtained, see [6], [7].

Concerning dihedral folding tilings by kites and an equilateral or isosceles triangle, the classification was obtained recently, see [1], [2], [3], [4]. In this paper we initiate the classification of dihedral folding tilings of the sphere by kites and scalene triangles: we shall obtain all the dihedral f-tilings of the sphere by kites and scalene triangles in which the shorter side of the kite is equal to the longest side of the triangle. Our aim is to obtain a complete classification of spherical f-tilings by any kite and any triangle.

We recall that a spherical kite K (Figure 1-I) is a spherical quadrangle with two congruent pairs of adjacent sides, which are distinct from each other. Let us denote by $(\alpha_1, \alpha_2, \alpha_1, \alpha_3)$, $\alpha_2 > \alpha_3$, the internal angles of K in cyclic order. The side lengths are denoted by a and b, with $b > a$. From now on T denotes a spherical scalene triangle with internal angles $\beta > \gamma > \delta$ and side lengths $c > d > e$, see Figure 1-II.

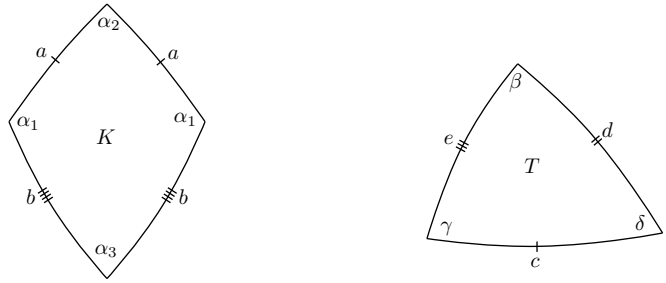

I II

Figure 1. A spherical kite K and a spherical scalene triangle T.

Taking into account the area of the prototiles K and T, we have

$$2\alpha_1 + \alpha_2 + \alpha_3 > 2\pi \quad \text{and} \quad \beta + \gamma + \delta > \pi.$$

As $\alpha_2 > \alpha_3$, we also have

$$\alpha_1 + \alpha_2 > \pi.$$

After certain initial assumptions are made, it is usually possible to deduce sequentially the nature and orientation of most of the other tiles. Eventually, either

a complete tiling or an impossible configuration proving that the hypothetical tiling fails to exist is reached. In the diagrams that follow, the order in which these deductions can be made is indicated by the numbering of the tiles. For $j \geqslant 2$, the location of tile j can be deduced directly from the configurations of tiles $(1, 2, \ldots, j-1)$ and from the hypothesis that the configuration is a part of a complete tiling, except where otherwise indicated.

We begin by pointing out that any f-tiling using K and T has at least two cells congruent to K and T, such that they are in adjacent positions and in one and only one of the situations illustrated in Figure 2.

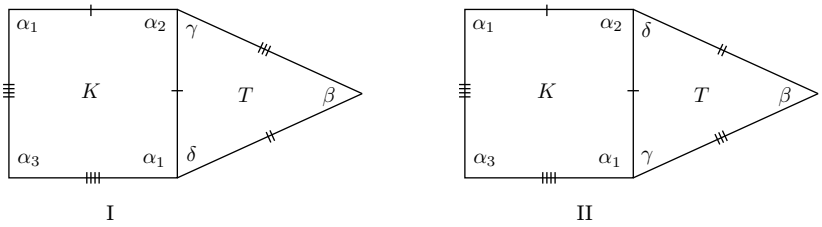

Figure 2. Distinct cases of adjacency.

Using spherical trigonometric formulas and $a = c$, we obtain

$$\frac{\cos\beta + \cos\gamma\cos\delta}{\sin\gamma\sin\delta} = \frac{\cos(\alpha_3/2) + \cos\alpha_1\ \cos(\alpha_2/2)}{\sin\alpha_1\sin(\alpha_2/2)}. \tag{1.1}$$

In this paper, the case of adjacency I will be addressed.

2. Case of Adjacency I

Suppose that any f-tiling using K and T has at least two cells congruent to K and T, such that they are in adjacent positions as illustrated in Figure 2-I.

Concerning the internal angles of the kite K, we have necessarily one of the following situations:

$$\alpha_1 \geqslant \alpha_2 > \alpha_3 \quad \text{or} \quad \alpha_2 > \alpha_1,\ \alpha_2 > \alpha_3$$

(the latter includes the cases $\alpha_2 > \alpha_1 \geqslant \alpha_3$ and $\alpha_2 > \alpha_3 > \alpha_1$).

The following propositions address these distinct cases.

Proposition A. *If $\alpha_1 \geqslant \alpha_2 > \alpha_3$, then there is an f-tiling using K and T if and only if*

$$\alpha_1 + \delta = \pi, \quad \beta = \frac{\pi}{2}, \quad \alpha_2 + 2\gamma = \pi, \quad \alpha_1 + \alpha_3 = \pi \quad \textit{and} \quad \delta = \frac{\pi}{k},\ k \geqslant 3,$$

or

$$\alpha_1 + \delta = \pi, \quad \beta = \frac{\pi}{2}, \quad \alpha_2 + 2\gamma = \pi \quad \textit{and} \quad \alpha_3 = \frac{\pi}{k},\ k \geqslant 3.$$

In the first situation, for each $k \geqslant 3$, there exists a unique f-tiling, say $\mathcal{M}^k$, with $\gamma = \arcsin(\cos(\pi/k)/\cos(\pi/2k))$. A planar representation of $\mathcal{M}^k$ is illustrated in Figure 9. For 3D representations of $\mathcal{M}^3$ and $\mathcal{M}^4$ see Figure 10.

In the second situation, the angles γ and δ satisfy $\cos\delta = \cos(\pi/2k)\sin\gamma$ and, for each $k \geqslant 3$, there exists a continuous family of f-tilings, say $\mathcal{S}^k_\delta$, with $\delta \in \big(\delta^k_{\min}, \delta^k_{\max}\big)$, where

$$\delta^k_{\min} = \arccos\Big(\cos^2\frac{\pi}{2k}\Big) \quad \textit{and} \quad \delta^k_{\max} = \arctan\frac{1}{\cos(\pi/2k)}.$$

Equivalently, we have that $\gamma \in (\delta^k_{\max}, (k-1)\pi/2k)$. A planar representation of $\mathcal{S}^k_\delta$ is illustrated in Figure 12. For 3D representations of $\mathcal{S}^3_\delta$, $\mathcal{S}^4_\delta$ and $\mathcal{S}^5_\delta$ see Figure 14.

P r o o f. Suppose that any f-tiling using K and T has at least two cells congruent to K and T, such that they are in adjacent positions as illustrated in Figure 2-I and $\alpha_1 \geqslant \alpha_2 > \alpha_3$ ($\alpha_1 > \pi/2$).

With the labeling of Figure 3-I, we have

$$\theta_1 = \beta \quad \text{or} \quad \theta_1 = \delta.$$

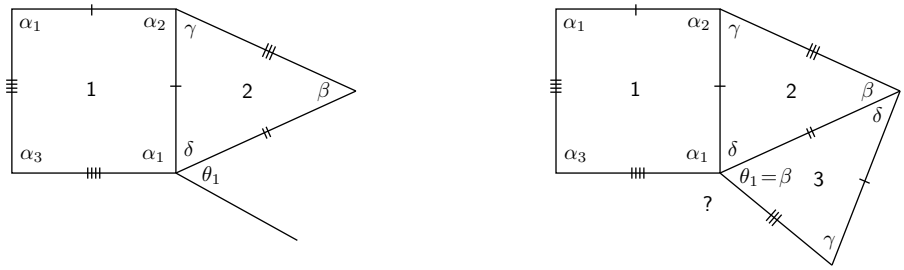

Figure 3. Local configurations.

A.1. Suppose first that $\theta_1 = \beta$. Then, we have necessarily $\alpha_1 + \beta < \pi$, as the case $\alpha_1 + \beta = \pi$ leads to an incompatibility between sides (see Figure 3-II).

Assuming $\alpha_1 + \beta < \pi$, we have necessarily $\alpha_1 + \beta + k\alpha_3 = \pi$ for some $k \geqslant 1$. As before, we are led to an incompatibility between sides; see Figure 4-I.

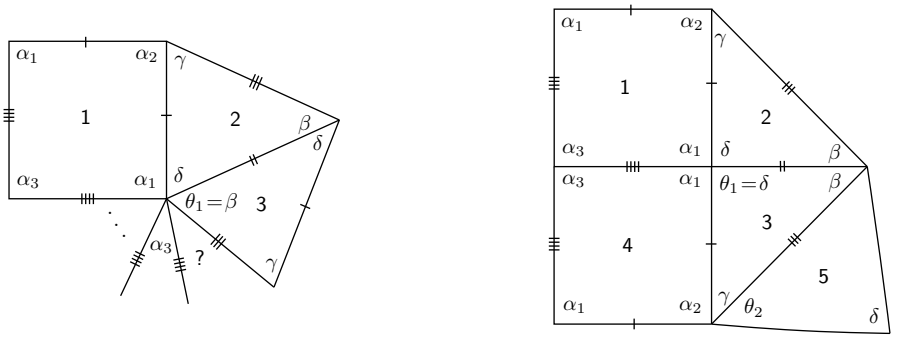

Figure 4. Local configurations.

A.2. Suppose now that $\theta_1 = \delta$ (Figure 3-I). Then we must have $\alpha_1 + \delta = \pi$ or $\alpha_1 + \delta < \pi$.

A.2.1. If $\alpha_1 + \delta = \pi$ (Figure 4-II), then, taking into account the edge lengths, we reach a vertex surrounded by the cyclic sequence of angles $(\alpha_1, \alpha_1, \delta, \delta)$. With the labeling of this figure, we have

$$\theta_2 = \beta \quad \text{or} \quad \theta_2 = \gamma.$$

A.2.1.1. If $\theta_2 = \beta$, then $\alpha_2 + \beta = \pi$ or $\alpha_2 + \beta < \pi$.

A.2.1.1.1. First, suppose that $\alpha_2 + \beta = \pi$. In this case we also have $\gamma + \delta = \pi$ (forced by the side lengths). Now, in an adjacent vertex surrounded by $(\beta, \beta, \gamma, \ldots)$ we obtain $\beta + \gamma \leqslant \pi$ which is impossible (note that $\beta > \delta$).

A.2.1.1.2. Assuming $\alpha_2 + \beta < \pi$ (Figure 5-I), we observe that the vertex surrounded by $(\beta, \beta, \gamma, \ldots)$ must have valency four, otherwise $\beta + \gamma + k\alpha_3 = \pi$ for some $k \geqslant 1$. But, in this case, an incompatibility between sides occurs. And so $\beta + \gamma = \pi$. On the other hand, as $\alpha_2 + \beta < \pi$, we get $\gamma > \alpha_2$, which determines tiles 7 and 8 (Figure 5-II). However, we reach a contradiction since $2\beta + \delta > \beta + \gamma + \delta > \pi$ (see side lengths).

A.2.1.2. We assume now that $\theta_2 = \gamma$ (Figure 4-II). Then we get $\beta + \beta \leqslant \pi$. If the equality is not satisfied, then $\beta + \beta + k\alpha_3 = \pi$ for some $k \geqslant 1$. But this situation leads to an incongruence among sides. Therefore, $\beta + \beta = \pi$, i.e., $\beta = \pi/2$ (Figure 6-I).

A.2.1.2.1. Suppose that $\alpha_2 + \gamma = \pi$. Then, we obtain the local configuration illustrated in Figure 6-II, where $\alpha_1 + k\alpha_3 = \pi$ for some $k \geqslant 1$. In Figure 7, the planar configuration for $k > 1$ is represented. However, we have no way to avoid a vertex surrounded by three consecutive angles α_1, which is impossible since $\alpha_1 > \pi/2$. And so $\alpha_1 + \alpha_3 = \pi$, i.e., $\alpha_3 = \delta$. This information enables us to extend in a unique way

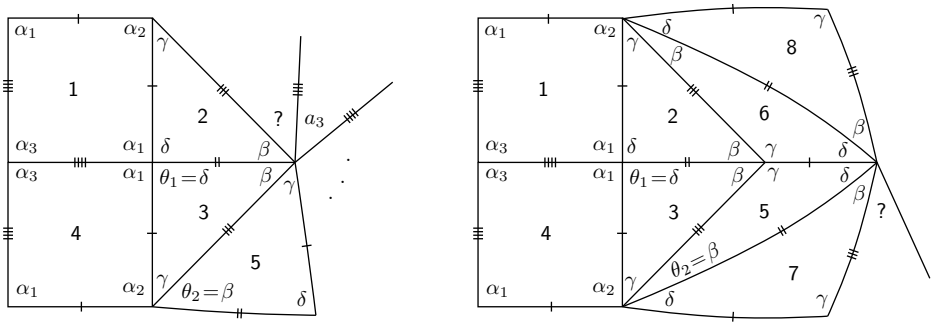

Figure 5. Local configurations.

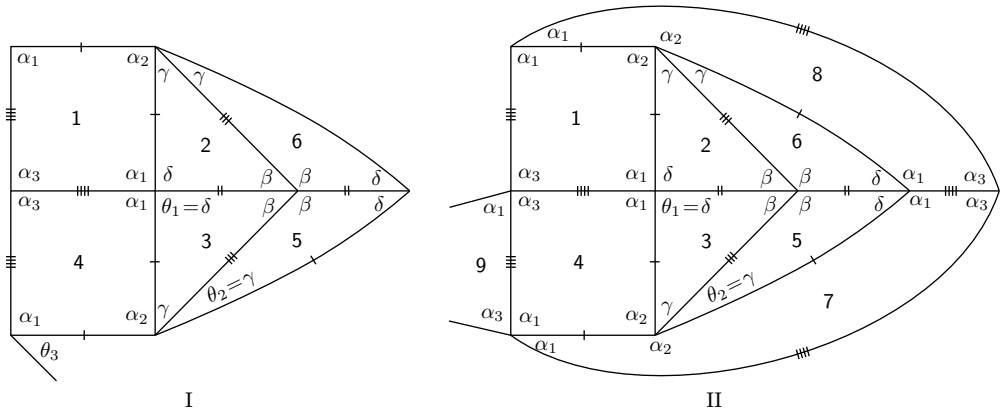

Figure 6. Local configurations.

the last configuration illustrated in Figure 6-II to get a closed one, where

$$\alpha_1 > \alpha_2 > \beta > \gamma > \alpha_3 = \delta,$$
$$\text{with} \quad \alpha_1 + \delta = \pi, \quad \beta = \frac{\pi}{2}, \quad \alpha_2 + \gamma = \pi \quad \text{and} \quad \alpha_1 + \alpha_3 = \pi.$$

As $0 < \delta < \gamma < \pi/2$, by (1.1) we have

$$\begin{aligned}
\frac{\cos(\pi/2) + \cos\gamma\cos\delta}{\sin\gamma\sin\delta} &= \frac{\cos(\delta/2) + \cos(\pi-\delta)\cos((\pi-\gamma)/2)}{\sin(\pi-\delta)\sin((\pi-\gamma)/2)} \\
&\Leftrightarrow \frac{\cos\gamma\cos\delta}{2\sin(\gamma/2)} = \cos\frac{\delta}{2} - \cos\delta\sin\frac{\gamma}{2} \\
&\Leftrightarrow \cos\delta\Big(\cos\gamma + 2\sin^2\frac{\gamma}{2}\Big) = 2\sin\frac{\gamma}{2}\cos\frac{\delta}{2} \\
&\Leftrightarrow \cos\delta - 2\sin\frac{\gamma}{2}\cos\frac{\delta}{2} = 0,
\end{aligned}$$

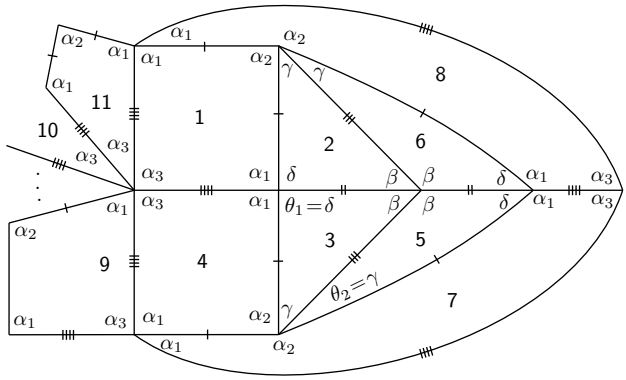

Figure 7. Local configurations.

which means that

$$\gamma = \gamma(\delta) = 2\arcsin\frac{\cos\delta}{2\cos\delta/2}.$$

In Figure 8, the graph of this function for $0 \leqslant \delta \leqslant \pi/2$ is outlined.

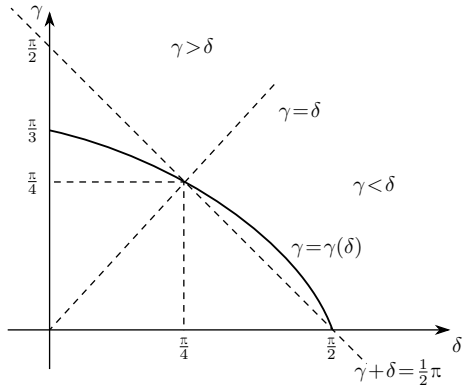

Figure 8. The function $\gamma = \gamma(\delta) = 2\arcsin(\cos\delta/(2\cos(\delta/2)))$.

Analysing the graph of the function $\gamma = \gamma(\delta)$, we conclude that there is no feasible region, since $\gamma + \delta > \pi/2$ and $\gamma > \delta$. And so, in this case, the closed planar representation does not correspond to a spherical f-tiling.

A.2.1.2.2. Suppose now that $\alpha_2 + \gamma < \pi$. With the labeling of Figure 6-I, we have necessarily

$$\theta_3 = \alpha_1 \quad \text{or} \quad \theta_3 = \delta.$$

A.2.1.2.2.1. Assuming $\theta_3 = \alpha_1$, we obtain $\alpha_1 + t\alpha_3 = \pi$ for some $t \geqslant 1$. We shall distinguish two distinct cases: $t = 1$ and $t > 1$.

A.2.1.2.2.1.1. For $t = 1$, the local configuration extends in a unique way to get the configuration illustrated in Figure 9 (observe that after tile 14 is placed, we get

$2\gamma + \alpha_2 \leqslant \pi$, and so $2\gamma + \alpha_2 + k\alpha_3 = \pi$, $k \geqslant 0$; however, if $k > 0$, we obtain an impossible configuration by analysis of the side lengths).

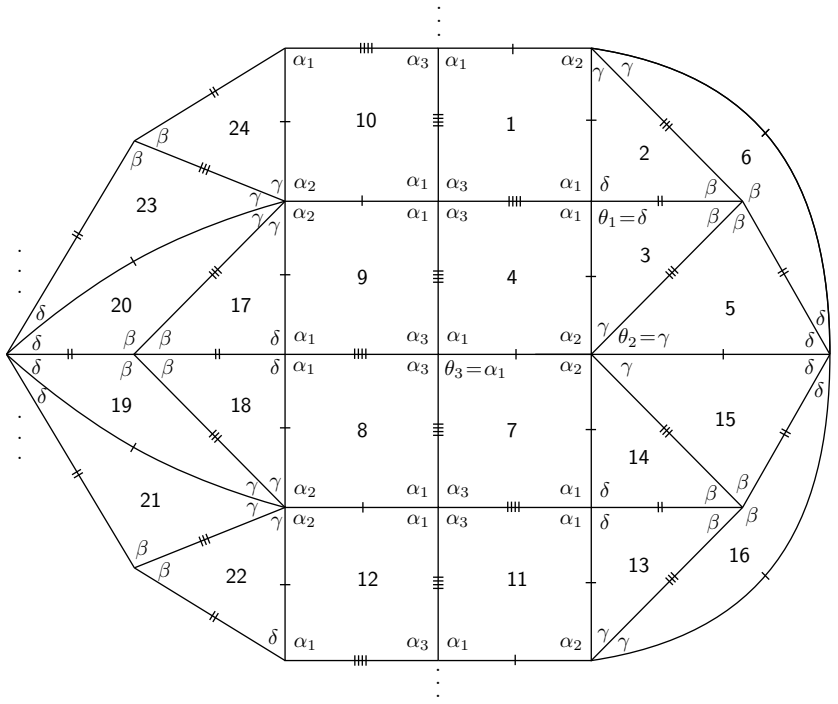

Figure 9. Planar representation.

In short, we have a planar representation in which the sums of alternate angles are

$$\alpha_1 + \delta = \pi, \quad \beta = \frac{\pi}{2}, \quad \alpha_2 + 2\gamma = \pi, \quad \alpha_1 + \alpha_3 = \pi \quad \text{and} \quad \delta = \frac{\pi}{k},\ k \geqslant 3.$$

As $0 < \pi/k = \delta < \gamma < \pi/2$, $k \geqslant 3$, using spherical trigonometry, we obtain

$$\frac{\cos\gamma\cos(\pi/k)}{\sin\gamma\sin(\pi/k)} = \frac{\cos(\pi/2k) - \cos(\pi/k)\sin\gamma}{\sin(\pi/k)\cos\gamma}$$
$$\Leftrightarrow\ \cos\frac{\pi}{k}\Big(\sin\gamma + \frac{\cos^2\gamma}{\sin\gamma}\Big) = \cos\frac{\pi}{2k}.$$

And so

$$\gamma = \arcsin\Big(\frac{\cos(\pi/k)}{\cos(\pi/2k)}\Big), \quad k \geqslant 3.$$

For $k = 3, 4, 5$ we obtain $\gamma \approx 35.26°$, $\gamma \approx 49.94°$ and $\gamma \approx 58.28°$, respectively. Observe that, if $k \geqslant 6$, then $\gamma > \pi/3 > \alpha_2$ (in fact, γ is increasing with k, and tends to $\pi/2$).

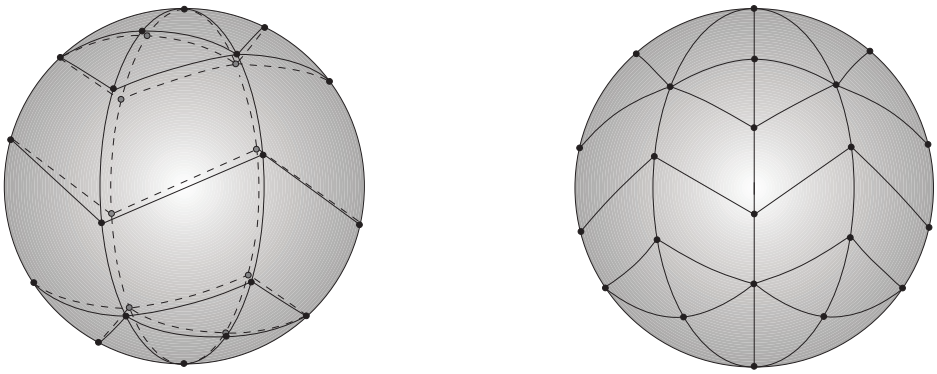

Figure 10. 3D representations of $\mathcal{M}^3$ and $\mathcal{M}^4$, respectively.

We shall denote such family of f-tilings by $\mathcal{M}^k$, $k \geqslant 3$. In Figure 10, 3D representations of $\mathcal{M}^3$ and $\mathcal{M}^4$ are illustrated ($x = 0$ is a line of symmetry).

A.2.1.2.2.1.2. If $t \geqslant 2$, we get the local configuration presented in Figure 11, which leads to a contradiction as we get three consecutive angles α_1 surrounding

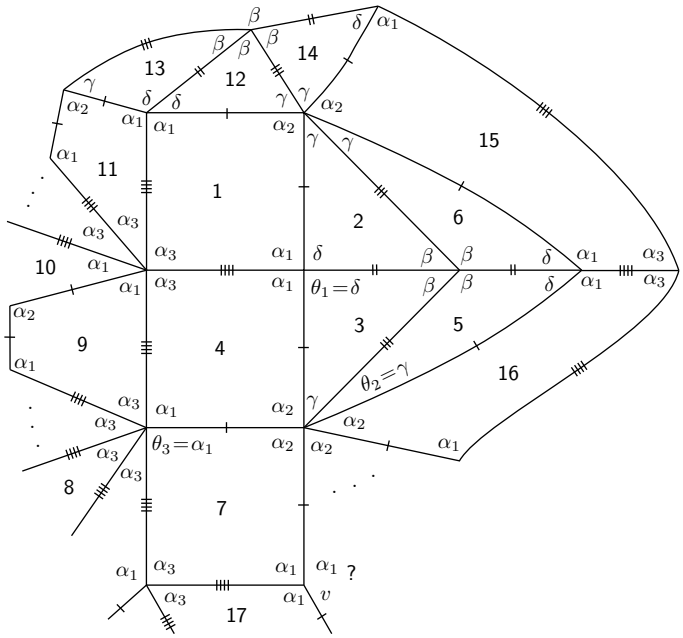

Figure 11. Local configuration.

a vertex. Observe that, as seen in the previous case, the situation $2\gamma + \alpha_2 \leqslant \pi$ implies $2\gamma + \alpha_2 = \pi$, by analysis of the side lengths, which determines tile 15. On the other hand, after tile 17 is placed, we obtain $2\alpha_2 + \gamma + \ldots = \pi$. Analysing the

side lengths, the remaining angles in this sum of alternate angles can only be α_2's (or nothing). However, this leads to an incongruence at vertex v since $\alpha_1 + \alpha_1 > \pi$.

A.2.1.2.2.2. Suppose now that $\theta_3 = \delta$ (Figure 6-I). It is a straightforward exercise to show that the local configuration extends in a unique way to get the configuration illustrated in Figure 12, where

$$\alpha_1 + \delta = \pi, \quad \beta = \frac{\pi}{2}, \quad \alpha_2 + 2\gamma = \pi \quad \text{and} \quad \alpha_3 = \frac{\pi}{k} \quad \text{for some } k \geqslant 3.$$

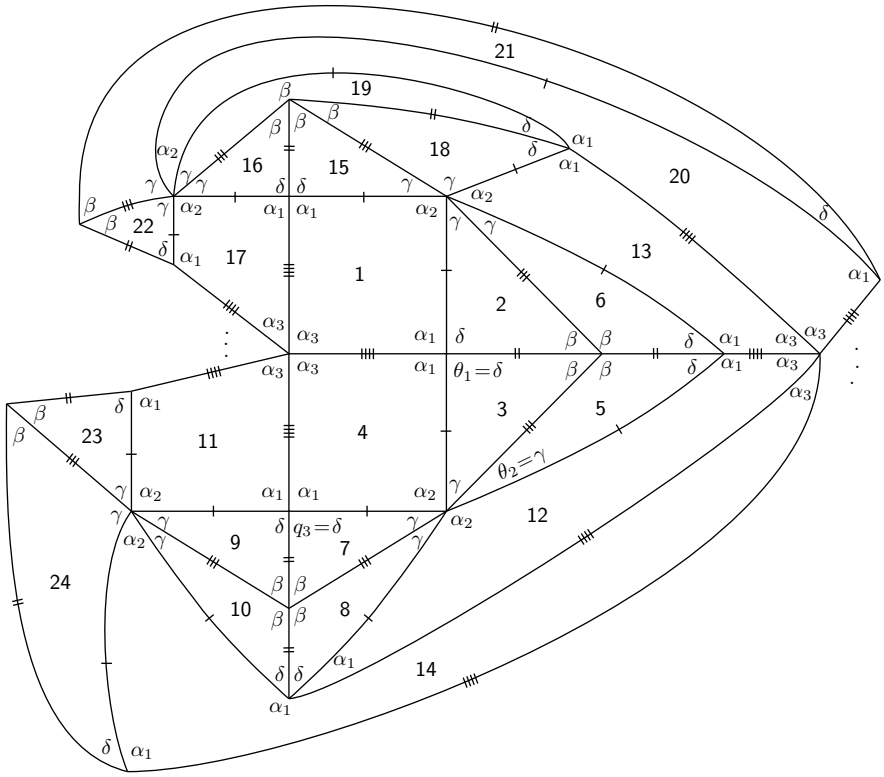

Figure 12. Planar representation.

Using (1.1), we obtain $\cos\delta = \cos(\pi/2k)\sin\gamma$, i.e.,

$$\gamma = \arcsin\frac{\cos\delta}{\cos(\pi/2k)}, \quad k \geqslant 3. \tag{2.1}$$

The above condition implies $\delta \geqslant \pi/2k$. In Figure 13, the graph of this function for $\pi/2k \leqslant \delta \leqslant \pi/2$ is outlined.

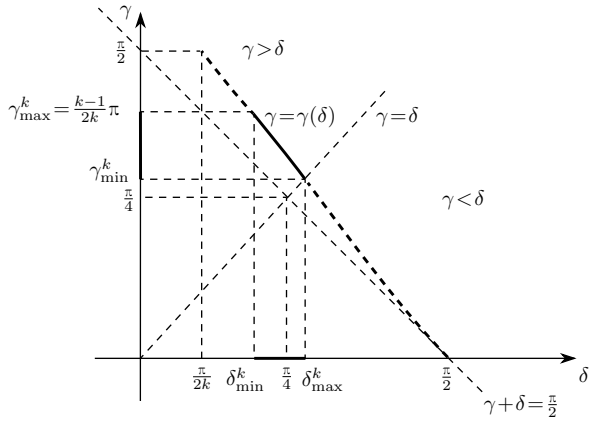

Figure 13. The function $\gamma = \gamma(\delta) = \arcsin(\cos\delta/\cos(\pi/2k))$, $k \geqslant 3$.

For any $\delta \in (\pi/2k, \pi/2)$, i.e., for any $\gamma \in (0, \pi/2)$, we may obtain an f-tiling whose planar representation is illustrated in Figure 12. However, it is not always within the scope of this paper. Using (2.1), we have

$$\alpha_2 > \alpha_3 \Leftrightarrow \pi - 2\gamma > \frac{\pi}{k} \Leftrightarrow \gamma < \frac{(k-1)\pi}{2k} = \gamma^k_{\max} \Leftrightarrow \delta > \arccos\Big(\cos^2\frac{\pi}{2k}\Big) = \delta^k_{\min}.$$

Moreover,

$$\delta < \gamma \Leftrightarrow \delta < \arctan\frac{1}{\cos(\pi/2k)} = \delta^k_{\max} \Leftrightarrow \gamma > \arctan\frac{1}{\cos(\pi/2k)} = \gamma^k_{\min}.$$

The cases $\alpha_2 = \alpha_3$ and $\delta = \gamma$ were studied in previous papers.

The values of $\delta^k_{\max} = \gamma^k_{\min}$ for $k = 3, 4$ and 20 are $49.1°$, $47.3°$ and $45.1°$, respectively. The values of $\delta^k_{\min}$ for $k = 3, 4$ and 20 are $41.4°$, $31.4°$ and $6.3°$, respectively.

We shall denote such family of f-tilings by $\mathcal{S}^k_\delta$, $k \geqslant 3$. Figure 14 illustrates $\mathcal{S}^3_\delta$, $\mathcal{S}^4_\delta$ and $\mathcal{S}^5_\delta$ (the reflection through the line $x = 0$ is a symmetry of $\mathcal{S}^k_\delta$).

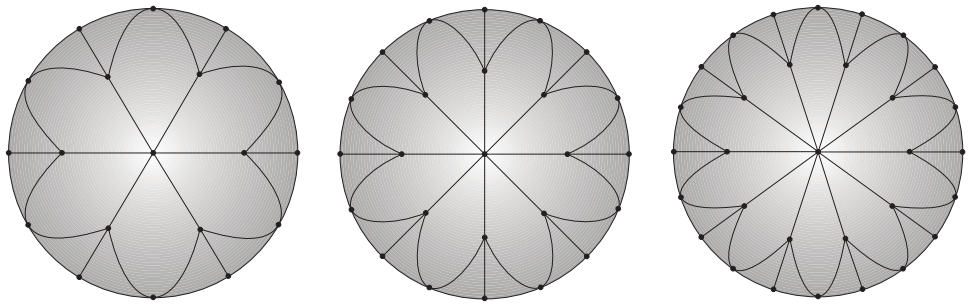

Figure 14. 3D representations of $\mathcal{S}^3_\delta$, $\mathcal{S}^4_\delta$ and $\mathcal{S}^5_\delta$, respectively.

A.2.2. Suppose now that $\alpha_1 + \delta < \pi$ (Figure 3-I). Taking into account the edge lengths, we get the local configuration illustrated in Figure 15-I, where

$$\theta_2 = \beta \quad \text{or} \quad \theta_2 = \gamma.$$

A.2.2.1. If $\theta_2 = \beta$, we shall obtain $\alpha_2 + \beta < \pi$. Note that if $\alpha_2 + \beta = \pi$, then we also have $\gamma + \delta = \pi$, by analysis of the side lengths. That is impossible (since $\beta > \gamma$ and $\alpha_2 > \delta$).

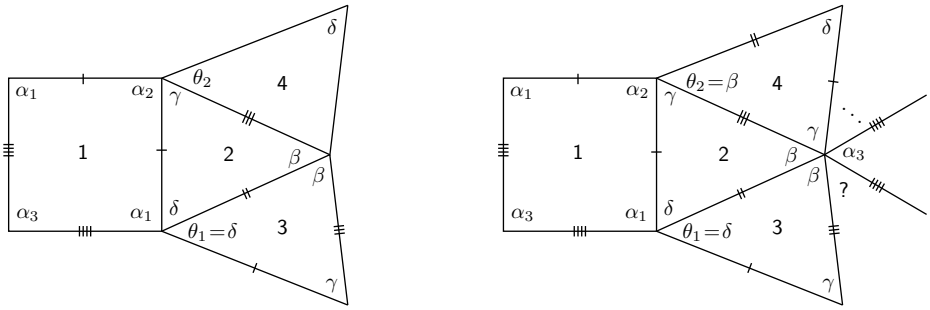

Figure 15. Local configurations.

With the labeling of Figure 15-II, the vertex surrounded by $(\beta, \beta, \gamma, \ldots)$ must satisfy $\beta + \gamma = \pi$, otherwise $\beta + \gamma + k\alpha_3 = \pi$ for some $k \geqslant 1$, which leads to an incompatibility between sides.

Now, as $\alpha_2 + \beta < \pi$ and $\beta + \gamma = \pi$, we have $\gamma > \alpha_2$. Such information allows us to extend the previous configuration to the one illustrated in Figure 16. We achieve a vertex surrounded by $(\beta, \beta, \beta, \ldots)$, which is a contradiction since $2\beta > \beta + \gamma = \pi$.

A.2.2.2. If $\theta_2 = \gamma$, then $2\beta \leqslant \pi$. Taking into account the edge lengths, we get $\beta = \pi/2$, leading us to the planar configuration illustrated in Figure 17-I. We shall distinguish

$$\alpha_2 + \gamma = \pi \quad \text{and} \quad \alpha_2 + \gamma < \pi.$$

A.2.2.2.1. First suppose that $\alpha_2 + \gamma = \pi$, $\alpha_1 \geqslant \alpha_2 > \beta = \pi/2 > \gamma > \delta$. This situation is presented in Figure 17-II. Considering the edge lengths, we get $\alpha_1 + k\alpha_3 = \pi$ for some $k \geqslant 1$ (note that δ cannot be part of this sum of alternate angles). On the other hand, we must have $\alpha_1 + t\delta = \pi$ for some $t \geqslant 2$, and consequently $3\gamma = \pi$ as illustrated in Figure 18. Now, one has $\alpha_1 \geqslant \alpha_2 = 2\pi/3$, and so $\delta \leqslant \pi/(3t) \leqslant \pi/6$. This implies $\beta + \gamma + \delta \leqslant \pi/2 + \pi/3 + \pi/6 = \pi$, which is impossible.

A.2.2.2.2. We assume now that $\alpha_2 + \gamma < \pi$. We shall distinguish two distinct situations, namely

$$\alpha_2 \geqslant \gamma \quad \text{and} \quad \alpha_2 < \gamma.$$

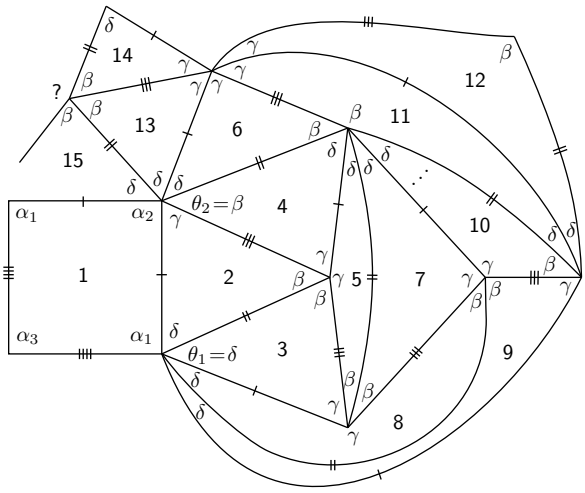

Figure 16. Local configuration.

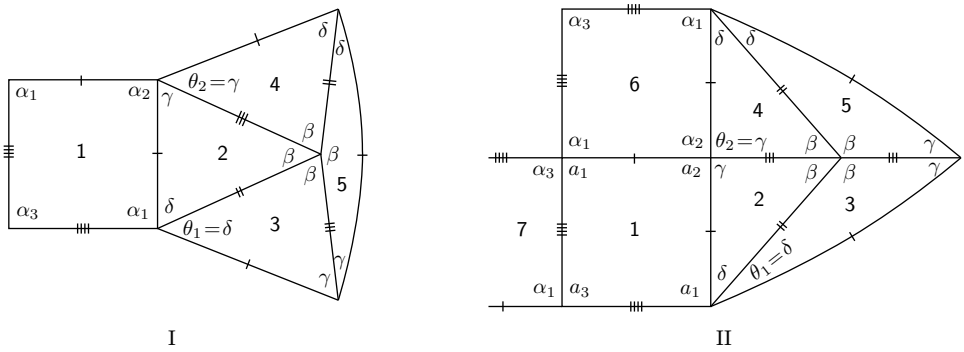

Figure 17. Local configurations.

A.2.2.2.2.1. First suppose that $\alpha_2 \geqslant \gamma$. According to the labeling of Figure 19-I, the angle x in tile 6 must satisfy

$$x = \alpha_3 \quad \text{or} \quad x = \alpha_2 \quad \text{or} \quad x = \gamma \quad \text{or} \quad x = \delta.$$

A.2.2.2.2.1.1. If $x = \alpha_3$, there exists $\varrho \in \{\alpha_1, \alpha_2, \gamma, \delta\}$ such that the sum of alternate angles not containing x (i.e., containing y) is $\alpha_1 + \gamma + \varrho > \beta + \gamma + \delta > \pi$, which is not possible.

A.2.2.2.2.1.2. If $x = \alpha_2$, we get the local configuration illustrated in Figure 19-II. It gives rise to a vertex surrounded by the cyclic sequence $(\alpha_1, \alpha_1, \delta, \delta, \ldots)$. Now, if $\alpha_1 + 2\delta \leqslant \pi$, then $\pi + \pi \geqslant (2\alpha_2 + \gamma) + (\alpha_1 + 2\delta) = (\alpha_1 + \alpha_2) + (\alpha_2 + \gamma + 2\delta) > 2\pi$, which is a contradiction. And so $\alpha_1 + \delta + k\alpha_3 = \pi$, $k \geqslant 1$. Taking into account the

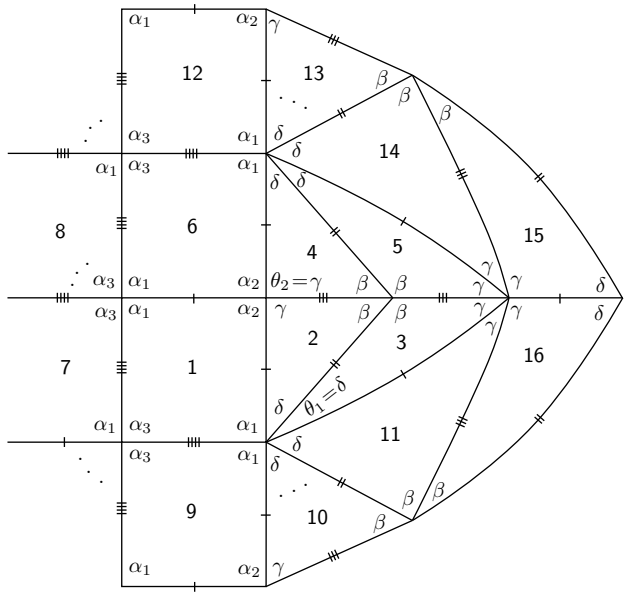

Figure 18. Local configuration.

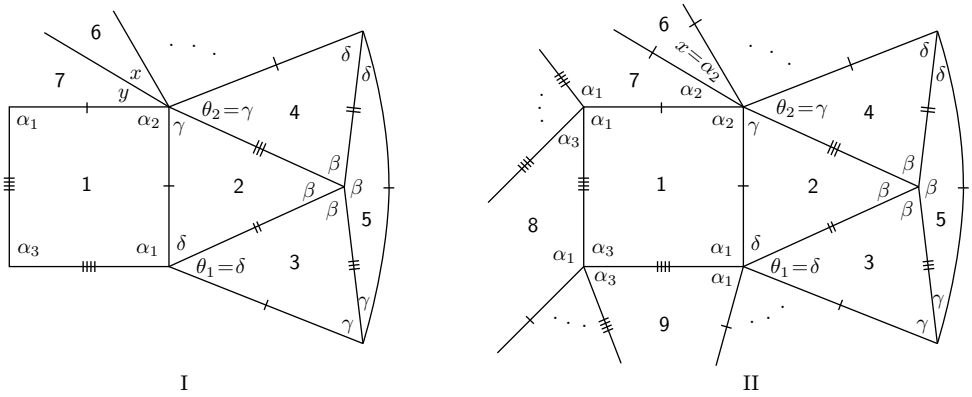

Figure 19. Local configurations.

side lengths, we must have one more angle α_1 around such a vertex, leading us to $2\alpha_1 \leqslant \pi$, which is impossible.

A.2.2.2.2.1.3. Suppose now that $x = \gamma$. Then we have $y = \alpha_2$ or $y = \gamma$. The first situation is similar to the previous case where $x = \alpha_2$, and also leads to a contradiction. Therefore, $y = \gamma$, i.e, $\gamma + \alpha_2 + \gamma \leqslant \pi$. Now, this sum of alternate angles cannot contain the angle δ as $\gamma + \alpha_2 + \gamma + \delta \geqslant 2(\gamma + \delta) > \pi$. On the other hand, if α_3 is part of this sum of alternate angles, then α_1 appears in the sum of

alternate angles containing y (by an analysis of the edge lengths), which is also not allowed. And so $\gamma + \alpha_2 + \gamma = \pi$.

On the other hand, we must have $\alpha_1 + \delta + \ldots = \pi$ (Figure 19-I). If two angles δ are part of this sum (i.e., $\alpha_1 + 2\delta \leqslant \pi$), then $2\pi \geqslant (\gamma + \alpha_2 + \gamma) + (\alpha_1 + 2\delta) = (\alpha_1 + \alpha_2) + (2\gamma + 2\delta) > 2\pi$, which is a contradiction. And so $\alpha_1 + \delta + k\alpha_3 = \pi$ for some $k \geqslant 1$, as illustrated in Figure 20-I. However, we get a vertex surrounded by three consecutive angles α_1, which is impossible.

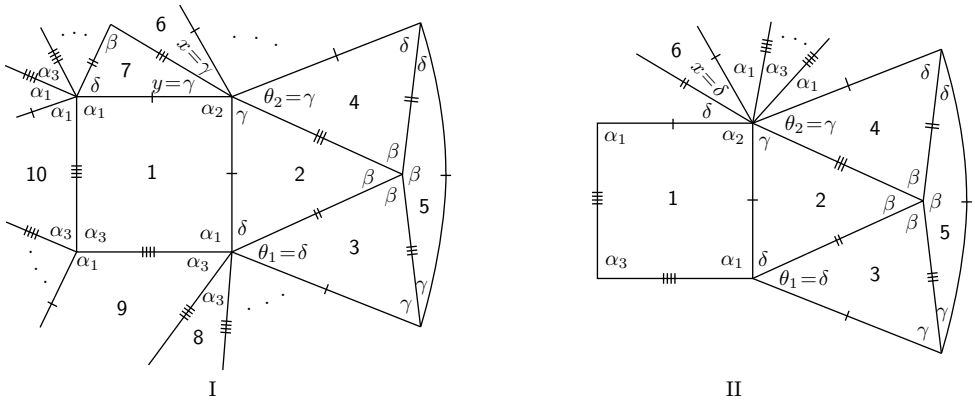

Figure 20. Local configurations.

A.2.2.2.2.1.4. Finally, we assume that $x = \delta$ (Figure 19-I). In this case we get $\alpha_2 + \gamma + \delta + k\alpha_3 = \pi$, $k \geqslant 0$.

Note that if $k \geqslant 1$, taking into account the edge lengths, the cyclic sequence of angles surrounding such a vertex is $(\alpha_1, \delta, \delta, \alpha_2, \gamma, \gamma, \alpha_1, \alpha_3, \ldots)$, as indicated in Figure 20-II. Adding all these angles, we obtain $2\alpha_1 + 2\gamma + 2\delta + \alpha_2 + \alpha_3 > 2\pi$, which is impossible.

Therefore, $k = 0$, i.e., $\alpha_2 + \gamma + \delta = \pi$, $\alpha_1 > \beta = \pi/2 > \alpha_2 \geqslant \gamma > \delta$. We will also distinguish two situations: $y = \delta$ and $y = \alpha_2$ (Figure 19-I).

A.2.2.2.2.1.4.1. If $y = \delta$, then we obtain $\alpha_1 + \gamma + t\alpha_3 = \pi$ for some $t \geqslant 0$, as illustrated in Figure 21-I. Supposing that $\alpha_1 + \gamma = \pi$ (i.e., $t = 0$), the union of the tiles 1, 2 and 7 is a spherical quadrilateral of area $\beta + \beta + \alpha_3 + (\alpha_1 + \delta) > 2\pi$, which means that $\alpha_1 + \delta + \alpha_3 > \pi$. And so, at vertices v_1 and v_2, we have $\alpha_1 + n\delta = \pi$ for some $n \geqslant 2$. Now, it follows that $\gamma = n\delta$ and we extend in a unique way the local configuration to obtain the one represented in Figure 21-II. From this we obtain $3\gamma \leqslant \pi$, leading us to the conclusion that $\beta + \gamma + \delta \leqslant \pi/2 + \pi/3 + \pi/(3n) \leqslant \pi$, since $n \geqslant 2$. This is a contradiction.

If $\alpha_1 + \gamma + t\alpha_3 = \pi$, with $t \geqslant 1$, then $\alpha_1 > \beta = \pi/2 > \alpha_2 > \gamma > \delta > \alpha_3$, and we get the local configuration illustrated in Figure 22, where $3\gamma = \pi$.

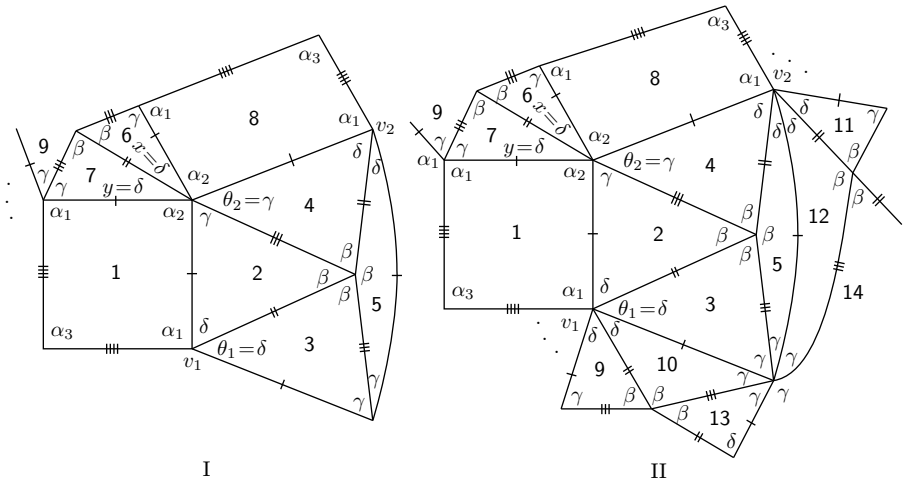

Figure 21. Local configurations.

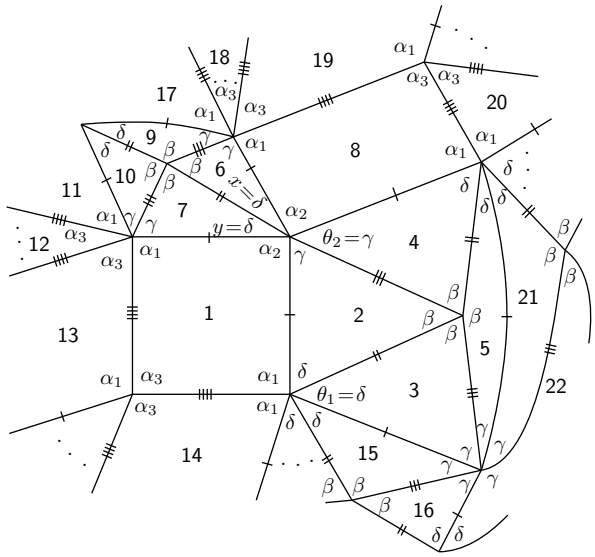

Figure 22. Local configuration.

Now, one gets $\alpha_1 + \alpha_1 + \alpha_2 + \alpha_3 < 2\pi/3 + 2\pi/3 + \alpha_2 + \delta < 4\pi/3 + 2\pi/3 = 2\pi$, which is impossible.

A.2.2.2.2.1.4.2. If $y = \alpha_2$, we also have $\alpha_1 + \gamma \leqslant \pi$ and $\alpha_1 + n\delta = \pi$ for some $n \geqslant 2$, as illustrated in Figure 23-I. As $\alpha_2 > \gamma$, the tile labeled by 15 is also completely determined. This information allows us to conclude that $\gamma = \pi/3$ (see the vertex surrounded by six angles γ).

Now, if $\alpha_1 + \gamma = \pi$, then $\gamma = n\delta$. This implies $\beta + \gamma + \delta \leqslant \pi$, which is impossible. Therefore, $\alpha_1 + \gamma + t\alpha_3 = \pi$, with $t \geqslant 1$, and we get the local configuration illustrated in Figure 23-II. However, there is no way to avoid a vertex surrounded by $(\alpha_1, \alpha_3, \alpha_1, \ldots)$, which is impossible.

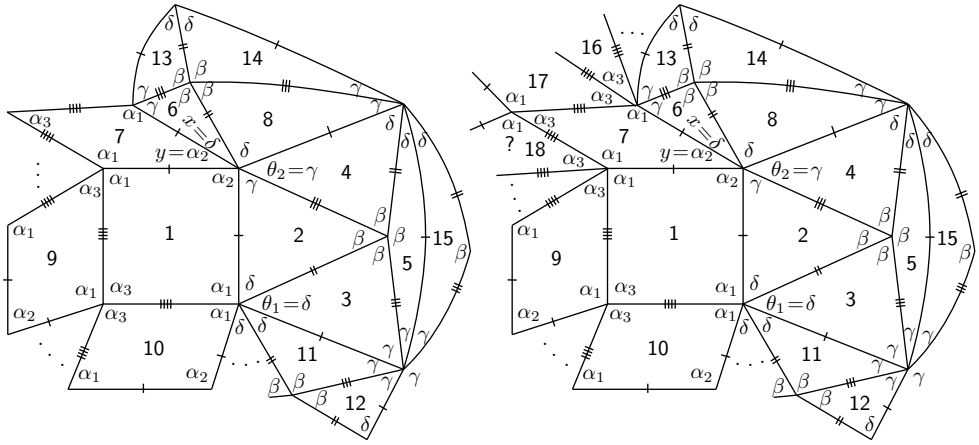

Figure 23. Local configurations.

A.2.2.2.2.2. Now we shall suppose that $\gamma > \alpha_2$. Recall that we also have $\alpha_1 + \delta < \pi$ and $\alpha_2 + \gamma < \pi$.

With the labeling of Figure 24-I, we begin by assuming that tile 6 is a spherical kite. In this situation, taking into account the edge lengths, we must have $\alpha_1 + \delta + k\alpha_3 = \pi$

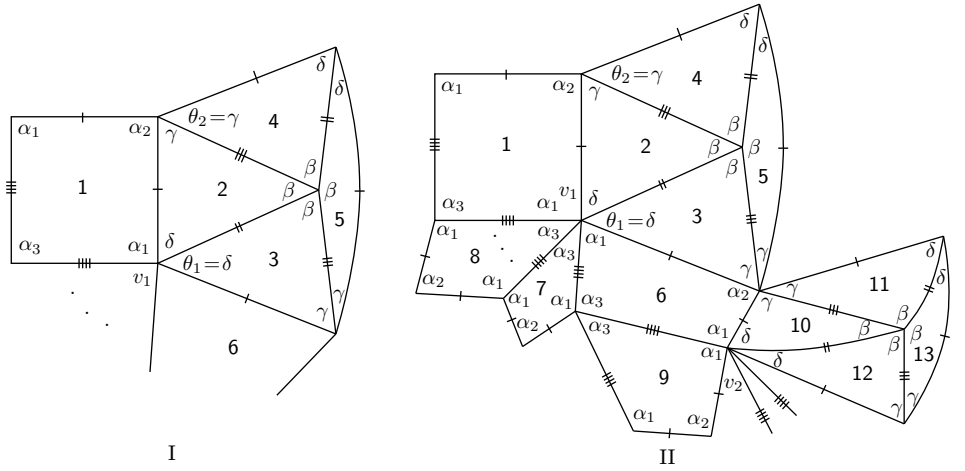

Figure 24. Local configurations.

for some $k \geqslant 1$ (vertex v_1). On the other hand, as $\gamma > \alpha_2$, we have $\alpha_1 + \gamma > \pi$, leading us to the conclusion that $\gamma + \alpha_2 + \gamma \leqslant \pi$ as indicated in Figure 24-II. Now, if $\alpha_1 + 2\delta \leqslant \pi$, then $2\pi \geqslant (2\gamma + \alpha_2) + (\alpha_1 + 2\delta) = (\alpha_1 + \alpha_2) + (2\gamma + 2\delta) > 2\pi$, which is a contradiction. And so we also have $\alpha_1 + \delta + k\alpha_3 = \pi$ around vertex v_2. However, taking into account the edge lengths, we will obtain (at least) three angles α_1 surrounding v_2, leading to a contradiction ($\alpha_1 + \alpha_1 > \pi$).

Suppose now that tile 6 is a spherical triangle. Then, it is a straightforward exercise to see that it is uniquely positioned as indicated in Figure 25-I. We also obtain $\alpha_1 + 2\delta \leqslant \pi$ and $2\gamma < \pi$. Now, if $3\gamma \leqslant \pi$ or $2\gamma + \alpha_2 \leqslant \pi$, then similarly to previous cases we get a contradiction (note that we are assuming $\gamma > \alpha_2$). And so $2\gamma + \delta + t\alpha_3 = \pi$, $t \geqslant 0$. Taking into account the side lengths, we must have $t = 0$, i.e., $2\gamma + \delta = \pi$. The planar configuration extends now to get the one illustrated in Figure 25-II (observe that tile 14 is uniquely determined, since $\gamma \neq \alpha_2$). It gives rise to a vertex surrounded by the cyclic sequence of angles $(\alpha_2, \gamma, \gamma, \delta, \delta, \delta, \delta, \ldots, \alpha_2)$, accordingly to the side lengths. A new vertex (say v) surrounded by $(\alpha_1, \gamma, \gamma, \ldots)$ appears, which is impossible, since $\alpha_1 + \gamma > \alpha_1 + \alpha_2 > \pi$. □

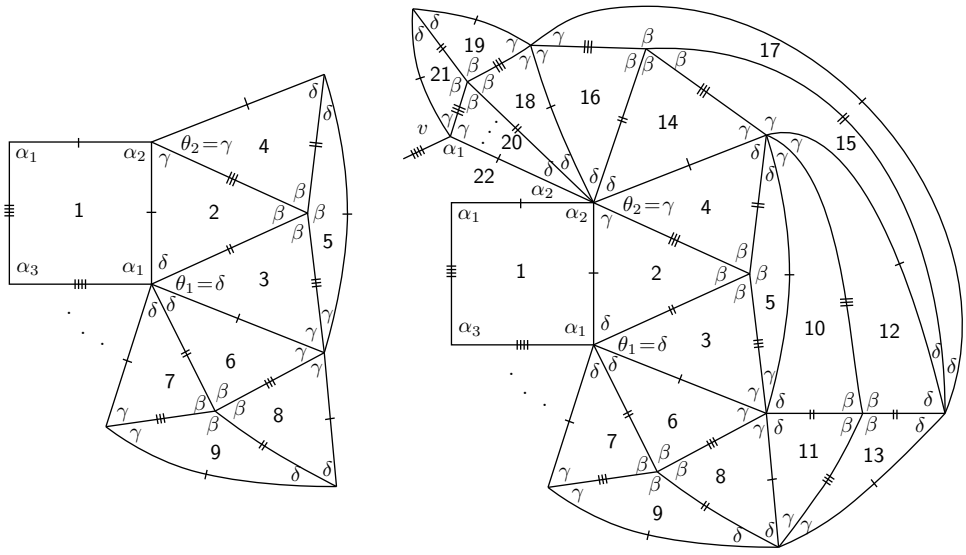

Figure 25. Local configurations.

Proposition B. *If $\alpha_2 > \alpha_1$, $\alpha_2 > \alpha_3$, then there is no f-tiling using K and T.*

P r o o f. Suppose that any f-tiling using K and T has at least two cells congruent to K and T, such that they are in adjacent positions as illustrated in Figure 2-I and $\alpha_2 > \alpha_1$, $\alpha_2 > \alpha_3$, $\alpha_2 > \pi/2$.

With the labeling of Figure 26-I, we have necessarily

$$\theta_1 = \beta \quad \text{or} \quad \theta_1 = \gamma.$$

B.1. Assume first that $\theta_1 = \beta$. Then, we must have $\alpha_2 + \beta = \pi$ or $\alpha_2 + \beta < \pi$.

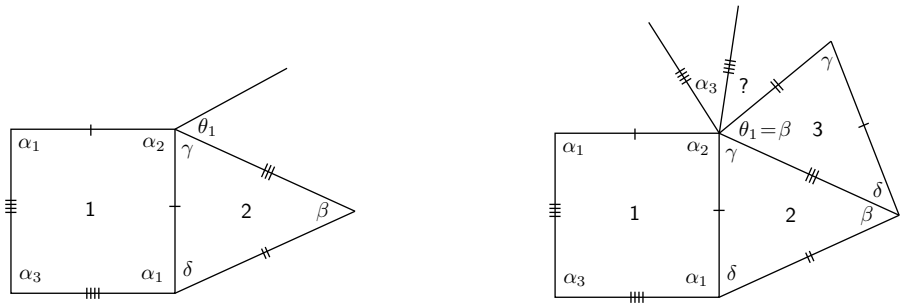

Figure 26. Local configurations.

B.1.1. If $\alpha_2 + \beta = \pi$, then we also have $\gamma + \delta = \pi$ by analysis of the side lengths. But this is not possible since $\beta > \gamma$ and $\alpha_2 > \delta$.

B.1.2. If $\alpha_2 + \beta < \pi$, then $\alpha_2 + \beta + k\alpha_3 = \pi$ for some $k \geqslant 1$. However, we get an incompatibility between sides (Figure 26-II).

B.2. Suppose now that $\theta_1 = \gamma$ (Figure 27-I). Then one gets $\alpha_2 + \gamma < \pi$ or $\alpha_2 + \gamma = \pi$.

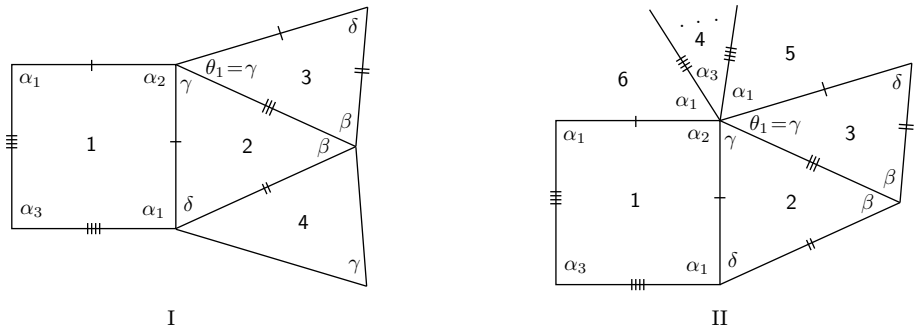

Figure 27. Local configurations.

B.2.1. Suppose first that $\alpha_2+\gamma < \pi$. If $\beta \geqslant \alpha_2$, then we have no way of positioning the angle β in tile 4, and so $\beta < \alpha_2$. This information implies that $\alpha_2 + \gamma + k\alpha_3 = \pi$ for some $k \geqslant 1$, as illustrated in Figure 27-II. Concerning the other sum of alternate angles around such a vertex, we have $\alpha_1 + \gamma + \alpha_1 + (k-1)\alpha_3 = \pi$, leading us to the

conclusion that $\alpha_1 < \pi/2$. Now, with respect to the internal angles of K, one gets $2\alpha_1 + (\alpha_2 + \alpha_3) < \pi + \pi = 2\pi$, which is impossible.

B.2.2. Supposing $\alpha_2 + \gamma = \pi$, $\alpha_2 > \alpha_1 > \gamma > \delta$, with the labeling of Figure 28-I, we must have

$$\theta_2 = \beta \quad \text{or} \quad \theta_2 = \delta.$$

B.2.2.1. Assume first that $\theta_2 = \beta$. The case $\alpha_1 + \beta = \pi$ leads to an incompatibility between sides, while the case $\alpha_1 + \beta < \pi$ implies $\alpha_1 + \beta + k\alpha_3 = \pi$ for some $k \geqslant 1$, as $\alpha_1 > \gamma$. However, again we get an incompatibility as illustrated in Figure 28-II.

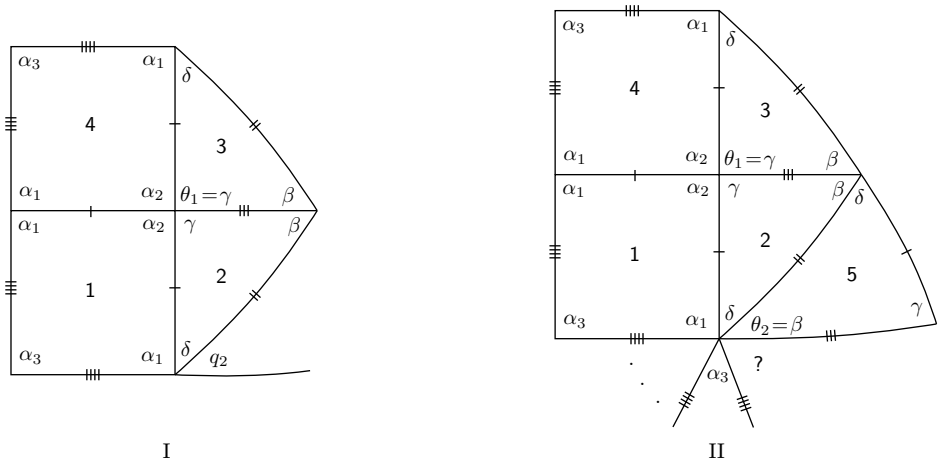

I II

Figure 28. Local configurations.

B.2.2.2. Suppose now that $\theta_2 = \delta$. In this situation we obtain the local configuration presented in Figure 29-I (observe that we must have $\beta = \pi/2$, otherwise we get an incompatibility between sides). It follows immediately that $\gamma + \delta > \pi/2$. Taking into account the area of the spherical kite K, we also observe that

$$\alpha_1 > \frac{\pi}{2} \quad \text{or} \quad \alpha_2 + \alpha_3 > \pi. \tag{2.2}$$

Now, with the labeling of Figure 29-I one has

$$\theta_3 = \alpha_2 \quad \text{or} \quad \theta_3 = \gamma \quad \text{or} \quad \theta_3 = \alpha_1 \quad \text{or} \quad \theta_3 = \delta.$$

B.2.2.2.1. Assuming that $\theta_3 = \alpha_2$, according to the edge lengths we have $\alpha_2 + \delta + \alpha_3 \leqslant \pi$, as indicated in Figure 29-II. And so, by (2.2), we get $\alpha_1 > \pi/2$. On the other hand, using again the edge lengths, we have no way to avoid at least two angles α_1 surrounding such a vertex, which is a contradiction.

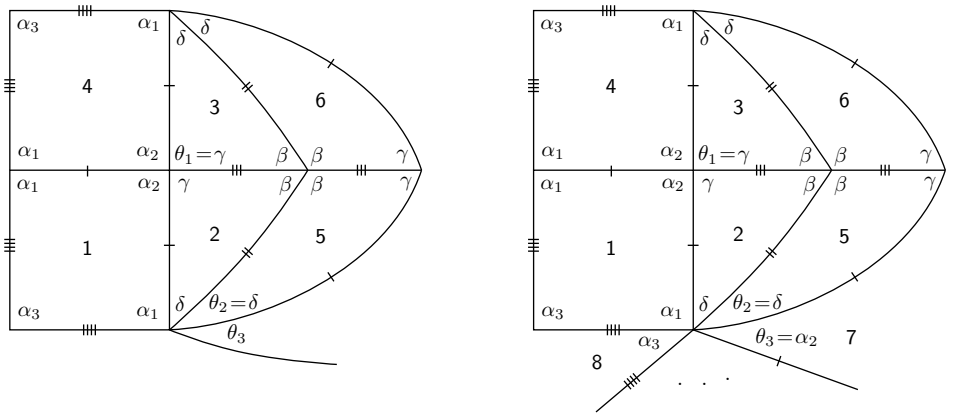

Figure 29. Local configurations.

B.2.2.2.2. Suppose that $\theta_3 = \gamma$ (Figure 30-I). After the tile labeled by 8 is placed, we conclude that $\alpha_1 + \gamma + \delta \leqslant \pi$. Therefore, $\alpha_1 < \pi/2$. Now, by (2.2), one gets $\alpha_2 + \alpha_3 > \pi$. And so

$$\alpha_2 > \alpha_3 > \gamma > \delta \quad \text{and} \quad \alpha_2 > \beta = \frac{\pi}{2} > \alpha_1 > \gamma > \delta.$$

It follows that $\alpha_1+\gamma+\delta+\varrho > 2\gamma+2\delta > \pi$ for all $\varrho \in \{\alpha_1, \alpha_2, \alpha_3, \beta, \gamma, \delta\}$. In order to verify the angle folding relation, we must have $\alpha_1 + \gamma + \delta = \pi$, which determines tile 9. We also get $\alpha_2 + k\delta = \pi$ for some $k \geqslant 2$.

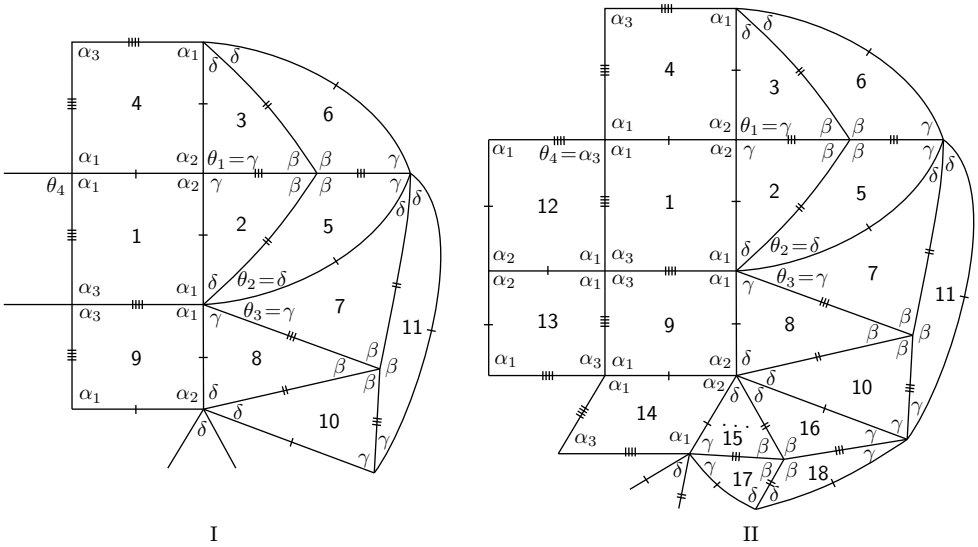

Figure 30. Local configurations.

With the labeling of Figure 30-I, if $\theta_4 = \alpha_1$, then $2\alpha_1 < \pi = \alpha_1 + \gamma + \delta < 2\alpha_1 + \delta$. And so we necessarily have $\theta_4 = \alpha_3$, as illustrated in Figure 30-II.

Now, $\alpha_1 + \alpha_3 + \delta > \alpha_1 + \gamma + \delta = \pi$ implies that $\alpha_1 + \alpha_3 = \pi$. This additional information allows us to write

$$\alpha_2 > \alpha_3 > \beta = \frac{\pi}{2} > \alpha_1 > \gamma > \delta.$$

As a result, we can determine tile 14 (and the remaining ones). It follows that $2\gamma + \alpha_1 > \pi > 2\gamma + \delta$, and so $3\gamma = \pi$. As $\gamma = k\delta$ for some $k \geqslant 2$, it follows that $\beta + \gamma + \delta = \pi/2 + \pi/3 + \pi/(3k) \leqslant \pi/2 + \pi/3 + \pi/6 = \pi$, which is impossible.

B.2.2.2.3. Suppose now that $\theta_3 = \alpha_1$. With the labeling of Figure 31, we have $\theta_4 = \alpha_3$ or $\theta_4 = \alpha_1$.

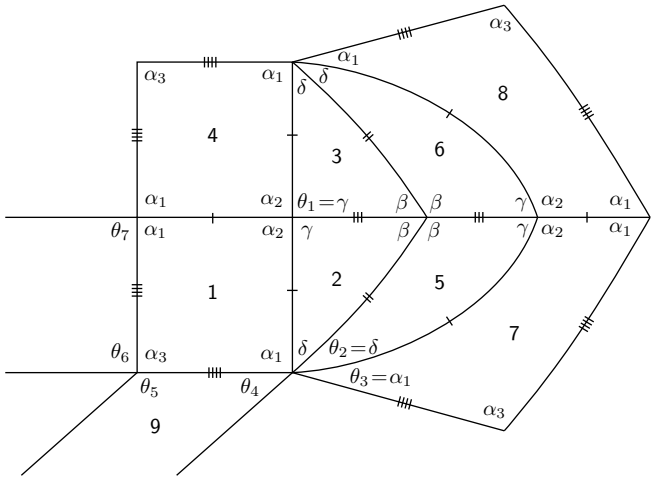

Figure 31. Local configuration.

B.2.2.2.3.1. If $\theta_4 = \alpha_3$, then, in order to fulfill the angle folding relation, we have $\alpha_1 + \delta + \alpha_3 \leqslant \pi$. As $\alpha_2 + \gamma = \pi$, then $\alpha_2 + \alpha_1 + (\gamma + \delta) + \alpha_3 \leqslant 2\pi$, which implies $\alpha_1 > \gamma + \delta > \pi/2$ (since $\alpha_2 + \alpha_1 + \alpha_1 + \alpha_3 > 2\pi$). Now, one has $\theta_5 = \alpha_1$, and $\theta_6 = \alpha_1$ or $\theta_7 = \alpha_1$, leading to a vertex with a sum of alternate angles containing two angles α_1, which is impossible.

B.2.2.2.3.2. If $\theta_4 = \alpha_1$ (see Figure 32), then, in order to verify the angle folding relation, we have $\alpha_1 + \delta + \alpha_1 \leqslant \pi$. As $\alpha_2 + \gamma = \pi$, we have $\alpha_2 + \alpha_1 + \alpha_1 + (\gamma + \delta) \leqslant 2\pi$, which implies $\alpha_3 > \gamma + \delta > \pi/2$. Now, one has $\alpha_2 > \alpha_3 > \beta = \pi/2 > \alpha_1 > \gamma > \delta$, which determines tile 10 and also implies $\alpha_3 + \alpha_1 = \pi$ and $\alpha_1 + \delta + \alpha_1 = \pi$.

This configuration gives rise to a vertex surrounded by the cyclic sequence of angles $(\alpha_3, \alpha_1, \delta, \delta, \delta, \ldots)$, with $\alpha_3 + k\delta = \pi$, $k \geqslant 2$. We immediately conclude that this leads to an incompatibility (by considering the edge lengths).

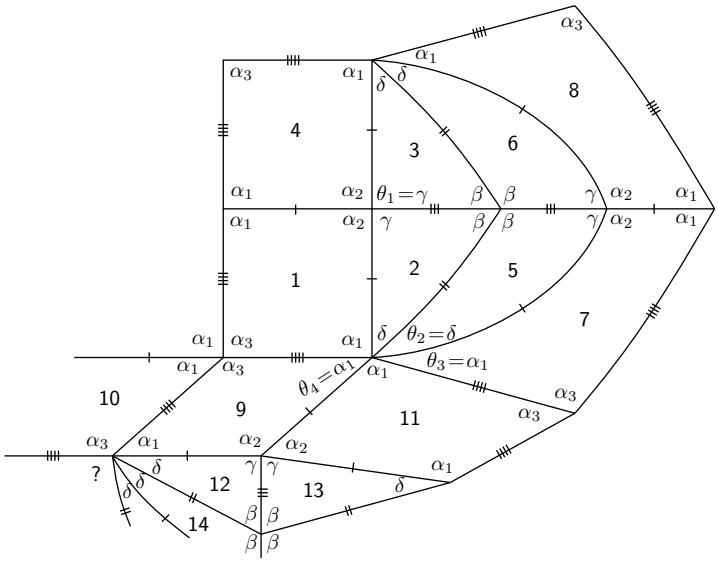

Figure 32. Local configuration.

B.2.2.2.4. Finally we will assume that $\theta_3 = \delta$. By the analysis of the previous cases we also assume $\theta_3' = \delta$ (Figure 33). This allows us to get $\gamma = \pi/3$; and, in short, we have $\alpha_2 = 2\pi/3 > \beta = \pi/2 > \gamma = \pi/3 > \delta > \pi/6$, $\alpha_2 > \alpha_1 > \gamma$ and $\alpha_2 > \alpha_3$.

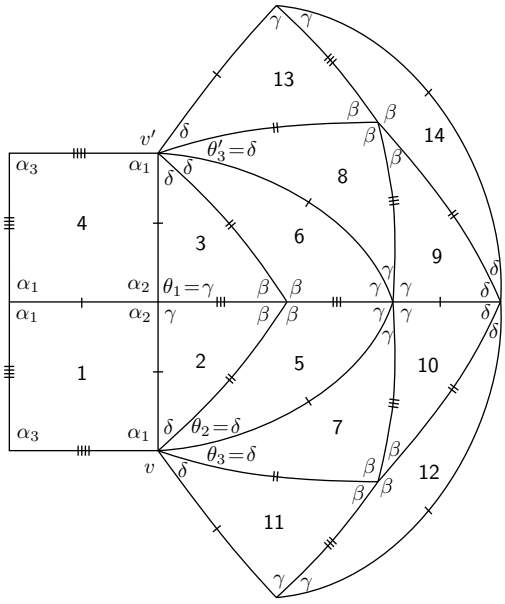

Figure 33. Local configuration.

With the labeling used in Figure 33, and in order to fulfill the angle folding relation, at vertices v and v', we have

$$\alpha_1 + k_1\delta + k_2\alpha_3 = \pi \quad \text{for some} \quad k_1 \geqslant 2 \quad \text{and} \quad k_2 \geqslant 0.$$

Now, if $k_2 > 0$, then $\alpha_1 + 2\delta + \alpha_3 \leqslant \pi$. On the other hand, we have $\alpha_2 + \gamma = \pi$ leading to $\alpha_2+\alpha_1+(\gamma+2\delta)+\alpha_3 \leqslant 2\pi$. And so $\alpha_1 > \gamma+2\delta > \pi/3+2\pi/6 = 2\pi/3 = \alpha_2$, which is a contradiction. Thus, we conclude that $k_2 = 0$. As $\alpha_1 > \pi/3$ and $\delta > \pi/6$, we also obtain

$$k_1 = 2 \quad \text{or} \quad k_1 = 3.$$

B.2.2.2.4.1. We shall assume first that $k_1 = 2$, i.e., $\alpha_1 + 2\delta = \pi$. With this assumption we easily get the local configuration presented in Figure 34, where

$$\theta_4 = \alpha_1 \quad \text{or} \quad \theta_4 = \alpha_3.$$

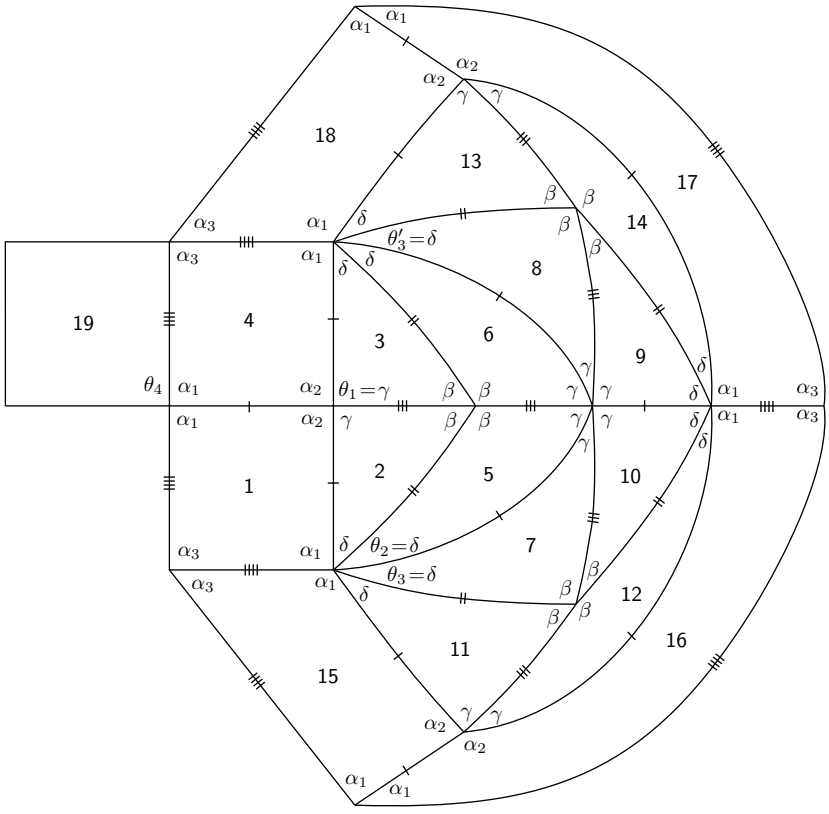

Figure 34. Local configuration.

B.2.2.2.4.1.1. If $\theta_4 = \alpha_1$, then $\alpha_1 \leqslant \pi/2$, and so $\alpha_2 + \alpha_3 > \pi$ (by (2.2)). This means that $\alpha_3 > \pi/3 > \delta$. Now, $2\alpha_1 + \delta > \alpha_1 + 2\delta = \pi$, leading us to the conclusion that $\alpha_1 = \pi/2$ (in order to fulfill the angle folding relation). On the other hand, if $2\alpha_3 + \delta = \pi$, one gets an incompatibility between sides. Therefore, we also have $\alpha_3 = \pi/2$. But is easy to verify that equation (1.1) is not satisfied for $\alpha_2 = 2\pi/3$, $\alpha_1 = \pi/2$, $\alpha_3 = \pi/2$, $\beta = \pi/2$, $\gamma = \pi/3$ and $\delta = \pi/4$.

B.2.2.2.4.1.2. Suppose now that $\theta_4 = \alpha_3$. In this situation, we get $\alpha_1 + \alpha_3 \leqslant \pi$. We shall see that it must be $\alpha_1 + \alpha_3 = \pi$. In fact,

(i) if $\alpha_1 \leqslant \pi/2$, $\alpha_1 > \gamma = \pi/3$, then $\alpha_2 + \alpha_3 > \pi$, i.e., $\alpha_3 > \pi/3$; now, as the sum of alternate angles $\alpha_1 + \alpha_3 + \delta = \pi$ leads to an incompatibility between sides, we get $\alpha_1 + \alpha_3 = \pi$;

(ii) if $\alpha_1 > \pi/2$, then $\alpha_1 + n\alpha_3 = \pi$ for some $n \geqslant 1$. The case $n > 1$ is illustrated in Figure 35 and also leads to a contradiction ($\alpha_2 + \gamma = \pi = \gamma + \gamma$); and so $\alpha_1 + \alpha_3 = \pi$.

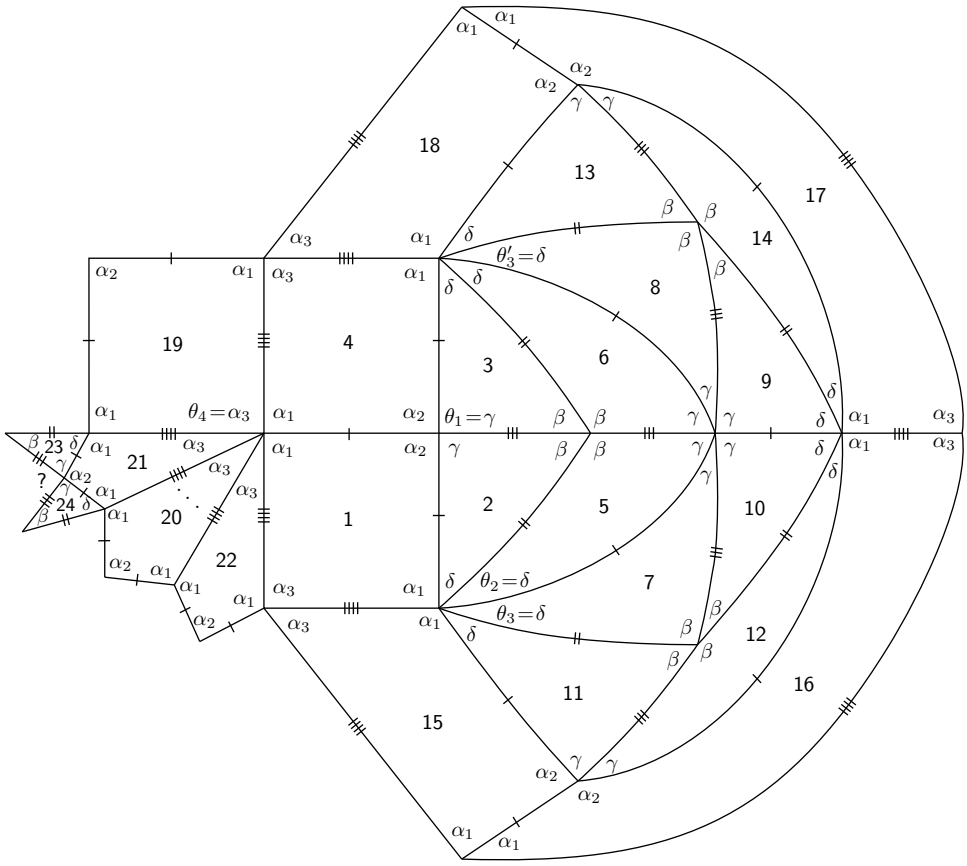

Figure 35. Local configuration.

In short, we have $\alpha_2 + \gamma = \pi$, $3\gamma = \pi$, $2\beta = \pi$, $\alpha_1 + 2\delta = \pi$ and $\alpha_1 + \alpha_3 = \pi$ (as the sums of alternate angles around vertices). Using now (1.1) for $\alpha_2 = 2\pi/3$, $\alpha_1 = \pi - 2\delta$, $\alpha_3 = 2\delta$, $\beta = \pi/2$ and $\gamma = \pi/3$, one gets $\delta = \pi/5 = 36^\circ$. We denote this f-tiling by $\mathcal{M}$. In Figure 36, the corresponding 3D representation is illustrated.

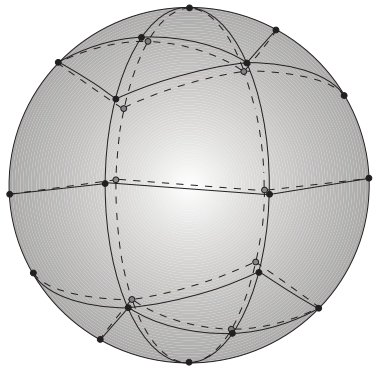

Figure 36. 3D representation of $\mathcal{M}$.

B.2.2.2.4.2. We suppose finally that $k_1 = 3$, i.e., $\alpha_1 + 3\delta = \pi$. With this assumption, we easily extend the previous local configuration (Figure 33) to the one presented in Figure 37 (from tile 15 to tile 36; note that, analogously to the previous case, we must have $\alpha_1 + \alpha_3 = \pi$). One gets a vertex surrounded by (at least) eight angles δ. As $\pi/6 < \delta < \pi/4$, in order to fulfill the angle folding relation, we must have $5\delta = \pi$ (by taking into account the edge lengths). And so,

$$\alpha_2 = \frac{2\pi}{3} > \alpha_3 = \frac{3\pi}{5} > \beta = \frac{\pi}{2} > \alpha_1 = \frac{2\pi}{5} > \gamma = \frac{\pi}{3} > \delta = \frac{\pi}{5}.$$

From here it is a straightforward exercise to show that this configuration extends in a unique way to obtain a closed one (with 100 tiles). However, such complete planar representation does not correspond to any f-tiling since the relation (1.1) fails. □

3. Combinatorial structure

Concerning the combinatorial structure of the f-tilings $\mathcal{M}^k$, $k \geqslant 3$, the group of symmetries that fix $(0, 0, 1)$ is the kth dihedral group D_k, generated by $R^z_{2\pi/k}$ (a rotation through an angle $2\pi/k$ around the z axis) and ϱ^{yz} (the reflection on the coordinate plane yz). In fact, neither the reflections on the vertical great circles bisecting triangles nor the rotations of the form $R^z_{(2n+1)\pi/k}$ ($n \in \mathbb{Z}$) are symmetries of $\mathcal{M}^k$. The map $a = R^z_{\pi/k}\varrho^{xy} = \varrho^{xy}R^z_{\pi/k}$ is a symmetry of $\mathcal{M}^k$ that maps $(0, 0, 1)$

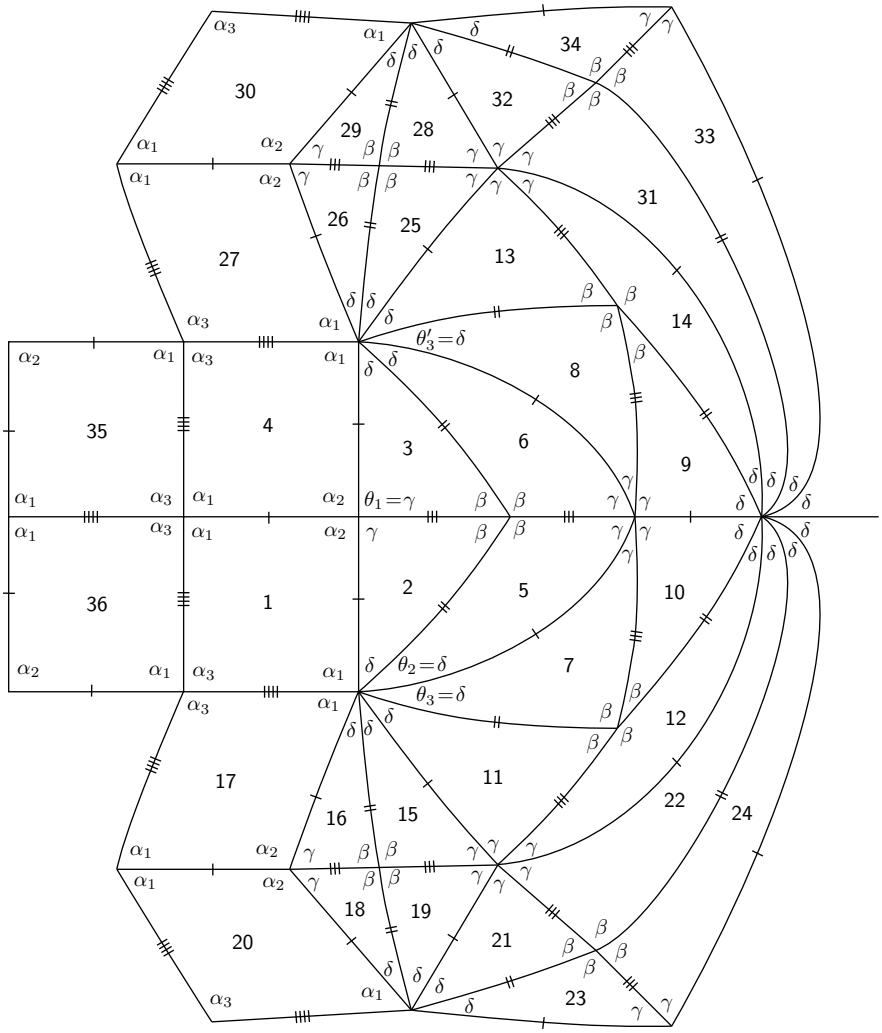

Figure 37. Local configuration.

into $(0,0,-1)$ allowing us to get all the symmetries that map $(0,0,1)$ into $(0,0,-1)$. Now, one has

$$a^{2k-1}\varrho^{yz} = R^z_{(2k-1)\pi/k}\varrho^{xy}\varrho^{yz} = R^z_{(2k-1)\pi/k}R^y_\pi = R^y_\pi R^z_{\pi/k} = \varrho^{yz}\varrho^{xy}R^z_{\pi/k} = \varrho^{yz}a.$$

On the other hand, a has order $2k$ and $\varrho^{yz} \notin \langle a\rangle$. It follows that a and ϱ^{yz} generate $G(\mathcal{M}^k)$ (the group of all symmetries of $\mathcal{M}^k$). And so it is isomorphic to D_{2k}. Finally, $\mathcal{M}^k$ has three transitivity classes of tiles, which means that $\mathcal{M}^k$ is 3-isohedral.

Concerning the combinatorial structure of the f-tilings $\mathcal{S}^k_\delta$, $k \geqslant 3$, we have that any symmetry of $\mathcal{S}^k_\delta$ fixes $(1,0,0)$ or maps $(1,0,0)$ into $(-1,0,0)$. The symmetries

that fix $(1,0,0)$ are generated by the rotation $R^x_{\pi/k}$ and the reflection ϱ^{xy}, giving rise to the dihedral group D_{2k}. The symmetries that map $(1,0,0)$ into $(-1,0,0)$ are obtained by composing each one of these elements with ϱ^{yz}. Since ϱ^{yz} commutes with $R^x_{\pi/k}$ and ϱ^{xy}, we conclude that $G(\mathcal{S}^k_\delta)$ is isomorphic to $C_2 \times D_{2k}$. It follows immediately that $\mathcal{S}^k_\delta$ is 2-isohedral.

It is now obvious that the group of all symmetries of $\mathcal{M}$ is isomorphic to D_6. Moreover, $\mathcal{M}$ has three transitivity classes of tiles and so it is 3-isohedral.

References

[1] *C. P. Avelino, A. F. Santos*: Spherical and planar folding tessellations by kites and equilateral triangles. Australas. J. Comb. *53* (2012), 109–125.

[2] *C. P. Avelino, A. F. Santos*: Spherical folding tesselations by kites and isosceles triangles II. Int. J. Pure Appl. Math. *85* (2013), 45–67.

[3] *C. P. Avelino, A. F. Santos*: Spherical folding tessellations by kites and isosceles triangles: a case of adjacency. Math. Commun. *19* (2014), 1–28.

[4] *C. P. Avelino, A. F. Santos*: Spherical folding tessellations by kites and isosceles triangles IV. Ars Math. Contemp. *11* (2016), 59–78.

[5] *A. M. Breda*: A class of tilings of S^2. Geom. Dedicata *44* (1992), 241–253.

[6] *A. M. Breda, R. Dawson, P. S. Ribeiro*: Spherical f-tilings by two noncongruent classes of isosceles triangles-II. Acta Math. Sin., Engl. Ser. *30* (2014), 1435–1464.

[7] *A. M. Breda, P. S. Ribeiro*: Spherical f-tilings by two non congruent classes of isosceles triangles-I. Math. Commun. *17* (2012), 127–149.

[8] *A. M. Breda, P. S. Ribeiro, A. F. Santos*: A class of spherical dihedral f-tilings. Eur. J. Comb. *30* (2009), 119–132.

[9] *A. M. Breda, A. F. Santos*: Dihedral f-tilings of the sphere by rhombi and triangles. Discrete Math. Theor. Comput. Sci. (electronic only) *7* (2005), 123–141.

[10] *R. J. M. Dawson*: Tilings of the sphere with isosceles triangles. Discrete Comput. Geom. *30* (2003), 467–487.

[11] *R. J. M. Dawson, B. Doyle*: Tilings of the sphere with right triangles. I: The asymptotically right families. Electron. J. Comb. *13* (2006), Research paper R48, 31 pages.

[12] *R. J. M. Dawson, B. Doyle*: Tilings of the sphere with right triangles. II: The $(1,3,2)$, $(0,2,n)$ subfamily. Electron. J. Comb. *13* (2006), Research paper R49, 22 pages.

[13] *S. A. Robertson*: Isometric folding of Riemannian manifolds. Proc. R. Soc. Edinb., Sect. A *79* (1977), 275–284.

[14] *Y. Ueno, Y. Agaoka*: Classification of tilings of the 2-dimensional sphere by congruent triangles. Hiroshima Math. J. *32* (2002), 463–540.

Authors' address: Catarina P. Avelino, Altino F. Santos, CMAT-UTAD, CEMAT-IST-UL, Universidade de Trás-os-Montes e Alto Douro, UTAD, Quinta de Prados, Vila Real 5001-801, Portugal, e-mail: `cavelino@utad.pt`, `afolgado@utad.pt`.